



# Probabilistic seismic hazard analysis (PSHA) for Ethiopia and the neighboring region



Atalay Ayele

Institute of Geophysics Space Science and Astronomy, Addis Ababa University, P.O.Box 1176, Addis Ababa, Ethiopia

## ARTICLE INFO

### Article history:

Received 13 July 2016

Received in revised form

11 May 2017

Accepted 22 June 2017

Available online 24 June 2017

### Keywords:

Probabilistic seismic hazard

Ethiopia

Horn of Africa

Seismicity

## ABSTRACT

Seismic hazard calculation is carried out for the Horn of Africa region ( $0^{\circ}$ – $20^{\circ}$  N and  $30^{\circ}$ – $50^{\circ}$  E) based on the probabilistic seismic hazard analysis (PSHA) method. The earthquakes catalogue data obtained from different sources were compiled, homogenized to  $M_w$  magnitude scale and declustered to remove the dependent events as required by Poisson earthquake source model. The seismotectonic map of the study area that avails from recent studies is used for area sources zonation. For assessing the seismic hazard, the study area was divided into small grids of size  $0.5^{\circ} \times 0.5^{\circ}$ , and the hazard parameters were calculated at the center of each of these grid cells by considering contributions from all seismic sources. Peak Ground Acceleration (PGA) corresponding to 10% and 2% probability of exceedance in 50 years were calculated for all the grid points using generic rock site with  $V_s = 760$  m/s. Obtained values vary from 0.0 to 0.18 g and 0.0–0.35 g for 475 and 2475 return periods, respectively. The corresponding contour maps showing the spatial variation of PGA values for the two return periods are presented here. Uniform hazard response spectrum (UHRS) for 10% and 2% probability of exceedance in 50 years and hazard curves for PGA and 0.2 s spectral acceleration ( $S_a$ ) all at rock site are developed for the city of Addis Ababa.

The hazard map of this study corresponding to the 475 return periods has already been used to update and produce the 3rd generation building code of Ethiopia.

© 2017 Published by Elsevier Ltd.

## 1. Introduction

The Afar Depression hosts a diffused triple junction where the Red Sea, Gulf of Aden and the East African divergent plate boundaries meet. Rifting along the Red Sea, Gulf of Aden and the East African Rift initiated around 29 Ma, apparently following weakening of the Nubia, Somalia and Arabia continental lithosphere (Fig. 1) caused by the Afar plume (e.g. McQuarrie et al., 2003; Garfunkel and Beyth, 2006). Crustal accretion at the three divergent plate boundaries typically occurs via episodic dike intrusions and magma dynamics manifested through earthquake occurrence and volcanic eruptions (Wright et al., 2006; Ayele et al., 2007, 2009; Keir et al., 2009; Ebinger et al., 2010). The Arabian plate is moving away from Nubia in a northeast direction in the Red Sea at a rate varying between 5.6 and 14 mm/yr along the strike of the rift (McClusky et al., 2009). Current estimates for spreading rates in the East African rift reach  $6 \pm 1.5$  mm/yr near the northernmost part in

the Ethiopian rift (Chu and Gordon, 1999). The two oceanic rifts can be categorized as ultraslow spreading ridges from their characteristics and rate of opening (Dick et al., 2003). The notable transition from oceanic to continental prototype on dry land, in this part of the Afro-Arabian rift system makes the region a unique and natural ocean-ridge laboratory for earth scientists. This area is characterized by pronounced volcanism, which greatly influences the tectonics and geodynamics of the region that has vast environmental and social implications. The ongoing volcanic activity and earthquake hazard in Ethiopia and surrounding region poses threats to the local populations and the relatively fast growing infrastructure. However, this threat has not been given due attention, mainly because governments and concerned stakeholders give high priority to other natural hazards like drought and food security issues. In addition, the region has never experienced disastrous earthquake damage in the recent past.

Earthquakes have attracted human curiosity since ancient times, but the scientific study of earth tremors is a fairly recent attempt. Instrumental recordings of earthquakes were not made until the last quarter of the nineteenth century, and the primary mechanism

E-mail address: [atalay.ayele@aau.edu.et](mailto:atalay.ayele@aau.edu.et).

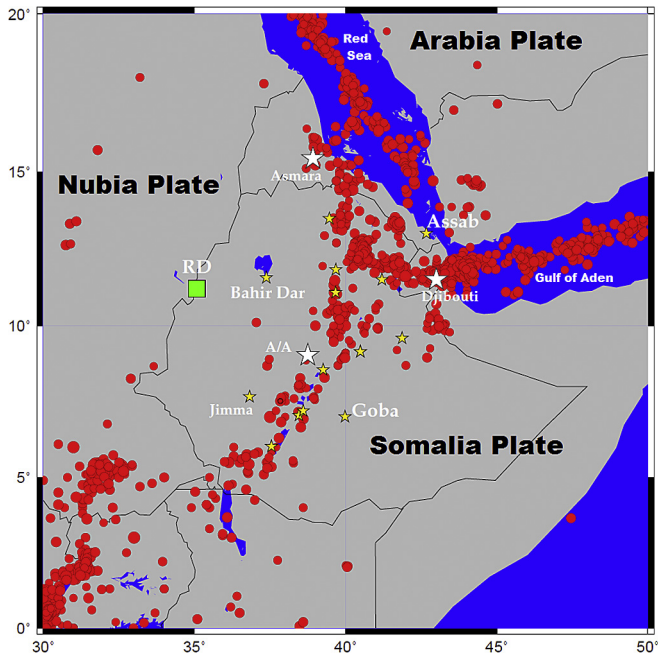


**Fig. 1.** Seismicity of the Horn of Africa region for the period from 1900 to 2012. The red spots are locations of earthquakes from the clustered catalogue where size of the circle is proportional with magnitude. The white stars show locations of capital cities in the region (A/A is to mean Addis Ababa) while the yellow stars show major towns in Ethiopia. There is an unintended overlap between urban centers and location of major earthquakes as most towns emerged from villages that developed over the years along the fertile rift valley for agriculture. The green square shows the location of the GERDP (Great Ethiopian Renaissance Dam Project) site.

for the generation of seismic waves, the release of accumulated strain by sudden slippage on a fault, was not widely recognized until the beginning of the twentieth century. The rise of earthquake science during the last hundred years illustrates how the field has progressed through a deep interplay among the disciplines of geology, physics, and engineering and yet we are unable to save the lives of thousands of victims during tremendous earthquake destruction where China is leading the death toll by over a million for the time period 1900 to 2016 (<https://www.statista.com>). Earthquakes also destroy massive and expensive infrastructures of nations that nearly paralyze the economy where Haiti is a case in point during the 2010 earthquake of magnitude 7.0  $M_w$  (DesRoches et al., 2011). We expect the worst in the years to come as the repeat times of large magnitude earthquakes are longer than the time coverage of instrumental earthquake catalogue. Historical earthquake catalogue and earthquake geology are assisting to date in bridging data gaps and making earthquake catalogues longer but the global coverage is sparse for several reasons.

Though at times earthquake hazard maps made with reasonable estimate fail (Stein et al., 2012), they are the solution to advise decision makers and investors so as to erect earthquake resistant structures with fair balance between cost and safety. Building earthquake hazard models is a process that evolves through time with the addition of more data and improved techniques. Model inputs come from earthquake catalogues, fault maps, ground motion prediction equations and slip rates (which can be estimated geodetically or from earthquake geology). Our knowledge in all these parameters is limited in scope and is even less accurate in developing countries. Due to these limitations, hazard maps often depend crucially on the authors' preconceptions, which can lead to significant over prediction or under prediction of hazards. Probably, no other branch of engineering has to deal with as much

uncertainly as earthquake engineering, e.g. recurrence of earthquakes, intensity of earthquakes, ground motion features, soil effects, topographic effects, structural properties, nonlinear dynamic behavior of structures, etc. On the other hand, the earthquake occurrence process is more complicated than the models assume which shows lack of comprehensive understanding of the complex earth processes.

The Tohoku (Japan) earthquake of March 2011 is the recent classic surprise for well prepared Japan (for mitigating earthquake risk) and the world at large where a magnitude 9.0 earthquake offshore generated a huge tsunami that overtopped sea walls, causing over 19,000 deaths and at least \$200 billion damage (Normile, 2012; Stein et al., 2012), including crippling nuclear power plants. Therefore there is no perfect earthquake hazard model even in the technologically advanced nations (Stein et al., 2012). The vulnerability to earthquake risk is even higher in developing countries which was well demonstrated by the classic examples of the 2010 earthquakes in Chile and Haiti. Countries that lie along the East African rift will not be an exception and there is a fear that destructive earthquakes may hit the fast growing cities located near the rift margins in Africa. With all these challenges, one has to produce and update the hazard model once every few years and hopefully use the updated maps to revisit building codes. For example, Ethiopia is one of the fastest growing countries in sub-Saharan Africa where the capital Addis Ababa is overwhelmed by a construction boom. However, the 2nd building code is over 20 years old and considerable earthquake activity has occurred ever since which is not considered in the current effort of erecting earthquake resistant structures. On top of the massive construction underway in the capital, Addis Ababa hosts the African Union (AU) headquarters and several other United Nations (UN) organizations. Therefore, moderate seismic activity corroborated by poor awareness makes the city risk level high. This demands a regular update of the seismic hazard map and building code of the country, which also applies for many others in the region.

Gouin (1976) produced the first seismic hazard map of Ethiopia using a probabilistic approach which served as a basis for developing the first building code of Ethiopia, ESCP-1:1983. Since the production of that map, quite a large number of destructive earthquakes occurred in the country causing damage both to property and human life. Consequently, Kebede and Asfaw (1996) revised the map and their results were used as an input into the second building code of the country, EBCS-8:1995. Kebede and Van Eck (1997) revisited the seismic hazard analysis for Ethiopia and neighboring countries with no much difference from Kebede and Asfaw (1996) both in approach and results but included spectral responses for some economically important cities and towns in the region. Both analyses by Kebede and Asfaw (1996) and Kebede and Van Eck (1997) were conducted for 100 years return period (i.e. 39.35% of being exceeded in 50 years), which is not the normal practice in building code revisions. In addition  $M_0$  (threshold magnitude) and b-values were assumed to be constant in all the 8 zones considered. Another probabilistic seismic hazard assessment for the sub-Saharan Africa was conducted by Midzi et al. (1999) for 10% probability of exceedance in 50 years but the source models are smoothed for regional scale, lacking detail compared to previous studies (Kebede and Asfaw, 1996; Kebede and Van Eck, 1997). All conducted studies in the region so far preferred to use the Poisson earthquake source model but proper catalogue declustering was not done with any one of the known algorithms which resulted in overestimation of the activity rate  $\lambda$  and hence the PGA (Peak Ground Acceleration) values.

A new probabilistic seismic hazard analysis has therefore been undertaken in this study to determine seismic ground motion parameters for seismic design of facilities located in the Horn of Africa

region that covers 0°N to 20°N Latitude and 30°E to 50°E Longitude (Fig. 1). It is evident from Fig. 1 that most of the major towns and capital cities in the region are located in the fertile rift valley for obvious reason which is a bad coincidence with elevated seismic risk in and around those areas. From the recorded history and instrumental catalogues, about 32 earthquakes of magnitude  $M_w \geq 6.2$  are known to have occurred in the study region as displayed in the Appendix. This list does not include the 1969 earthquake sequence in central Afar with maximum magnitude  $M_w$  6.1 that destroyed the town of Serdo, killing and injuring a substantial part of the population. The 1961 earthquake sequence in Kara Kore with maximum magnitude  $M_w$  6.5 severely damaged the nearby Majeti village (Gouin, 1979). During the 1989 Dobi graben (central Afar) earthquakes, several bridges on the highway connecting the port of Assab to Addis Ababa were destroyed. As a consequence, the highway link with the main sea port was disrupted creating scarcity of basic commodities in Addis Ababa and other large towns. Several moderate magnitude but widely felt earthquakes with minor damage occurred recently which need to be incorporated into the hazard model of the region. It is therefore prudent to assess potential earthquake hazard and produce maps that can provide information on the probable location and severity of possibly dangerous earthquakes and the likelihood of their occurrence in our area of interest.

## 2. PSHA methodology

The mitigation of earthquake risk through the use of seismic resistant design codes and effective urban planning is ultimately contingent on a good understanding of the seismic hazard on a site-specific, urban and regional scale. The methodology of probabilistic seismic hazard analysis (PSHA) is well established as a means of characterizing the level of ground motion to which a location may be subjected to within a given time period (Cornell, 1968, 1971; McGuire, 1976). There is a great deal of uncertainty about the location, size, and resulting shaking intensity of future earthquakes. Probabilistic Seismic Hazard Analysis (PSHA) aims to quantify these uncertainties, and combine them to produce an explicit description of the distribution of future shaking that may occur at a site of interest. In this approach, the seismic hazard is defined as the probability that a certain level of ground motion will be exceeded (at a given place and within a given time period). The last decade has witnessed the emergence of several freely available software packages for the calculation of seismic hazard (e.g., CRISIS (Ordaz et al., 2012); OpenSHA (Field et al., 2003)), which have helped to remove one of the key barriers preventing wider adoption of state-of-the-art seismic hazard analysis practices in many areas of the world. Crisis2012 software (Ordaz et al., 2012) is used in this study to carryout Probabilistic Seismic Hazard Analysis as the code is based on the standard Cornell (1968) approach. The PSHA model requires a seismic zonation model, characterization of each zone and a regional model for the seismic wave damping which is called the ground motion prediction equation (GMPE). Though there are limitations due to lack of data, model inputs implemented in this study are detailed below in the next section.

## 3. Data and model inputs

For ideal PSHA calculation, seismicity (earthquake geology, historical & instrumental), active fault database, strong ground motion database, strain rate database are required. However, the availability and quality of all these data varies from region to region to the extent that only an instrumental seismicity catalogue is used as in this study. The analysis started with the most updated available seismic catalog, to which careful completeness analyses and

declustering processes were applied as detailed below.

### 3.1. Seismicity data

An instrumentally recorded earthquake catalogue extending from 1900 to 2012 was merged together with previously existing ones for the Horn of Africa region (Gouin, 1979; Asfaw, 1986; Ayele, 1995) where each of them were compiled from a number of several other sources by avoiding overlaps and removing duplicates. Ayele (1995) covers the period 1960 to 1993. The data recorded from 1994 to 2012 are compiled for this study from national and ISC (International Seismological Centre) catalogues.

### 3.2. Magnitude homogenization

For characterization of seismicity of an area of interest or for comparison of earthquake activity occurring in different seismic regions, earthquake magnitude is one of the most commonly used descriptive source parameter. The most widely used magnitude scale is the local magnitude or Richter magnitude defined by Richter (1935). In most technical communications in seismological disciplines, several other magnitude types, including body wave magnitude ( $m_b$ ), surface wave magnitude ( $M_s$ ), and moment magnitude ( $M_w$ ) are commonly used. The moment magnitude scale is the most recent scale (Kanamori, 1977; Hanks and Kanamori, 1979) and is fundamentally different from the earlier scales. Rather than relying on measured seismogram amplitude peaks, the  $M_w$  scale is tied to the scalar seismic moment ( $M_0$ ) of an earthquake. The seismic moment magnitude thus more directly represents the amount of energy released at the source, rather than relying on the effects of that energy on one or more seismographs at some distance from the source. Hence  $M_w$  scale is the most preferred to use in seismic hazard calculation and other applications. Uncertainties associated with different magnitude types play a vital role during magnitude conversions. Very few studies have been devoted towards quantifying these uncertainties inherent in different magnitude scales and their scaling law. For seismological applications including homogenization of earthquake catalogs, it is essential to know how different magnitude determinations compare with each other and the associated measurement errors. Normally, relations linking the different magnitude scales are obtained through regression conversions following standard linear least squares approach (e.g. Scordilis (2006)). This approach is based on the assumption that one of the magnitudes (independent variable) is either error free or the order of its error is very small compared to the dependent variable measurement errors. Furthermore, the errors in the dependent variable are taken to be independent and normally distributed. Many empirical relationships have been developed in the past between various magnitude scales for mapping one type magnitude on to the other (Scordilis, 2006; Das et al., 2011). Attempt was made to find a reasonable regression relation for all earthquake magnitudes to  $M_w$  in the study area but the scatter was found to be large due to a limited dataset for regressing. We rather opted to use empirical relations from global data set (Scordilis, 2006; Das et al., 2011). Das et al. (2011) used orthogonally regressed magnitude conversion to a unified moment magnitude but the conversion overestimates relatively large magnitude events and underestimates smaller ones for our catalogue. As a result, we homogenized all earthquake magnitudes to  $M_w$  using Scordilis (2006) which is found to be reasonably stable.

### 3.3. PSHA model inputs

Poisson earthquake source model is the standard in PSHA and

risk calculations, which assumes that earthquake occurrence is independent of time and the past history of occurrences or nonoccurrence. The earthquake catalogue for this study is declustered using the [Gardner and Knopoff \(1974\)](#) algorithm where 1084 earthquakes of magnitude range  $3.0 \leq M_w \leq 7.2$  survived as independent events out of the original catalogue of 2644 earthquakes in the magnitude range  $3.0 \leq M_w \leq 7.2$  which is displayed on [Fig. 1](#).

In Ethiopia and its neighboring region, detailed Quaternary fault maps at a desirable scale indicating active faults are presently lacking and if they exist it is a challenge to associate them with observed seismicity. Earthquake locations in this tectonic regime have significant errors, on average about 50 kms, due to sparse seismic station distribution. Therefore, fault characteristics relevant for seismic hazard analysis, like fault geometry, slip direction and segmentation lengths are presently not available. If we succeed to associate observed seismicity to geologically mapped individual active faults, it is not easy to conclude whether the observed fault displacement is produced by a single earthquake or a cumulative effect of several previous earthquakes that occurred in the geologic past. However, our current knowledge about the tectonics and the seismicity is good enough to designate area source models within which earthquake characteristics may be taken to be uniform. A recent study conducted by [Hofstetter and Beyth \(2003\)](#) using regional geology, tectonics and seismicity, where several area sources are identified and characterized, is slightly modified using additional seismicity & fault plane solutions to identify 13 zones ([Fig. 2](#)). The seismic characteristics of the 13 area sources were modeled with the application of the Poisson source process where the Gutenberg-Richter (GR) magnitude-frequency distribution ([Gutenberg and Richter, 1944](#)) was employed for each individual zone.

$$\log N(M) = a - bM \quad (1)$$

Where  $N(M)$  is the cumulative number of earthquakes or at times called the rate of earthquakes with magnitude  $M \geq M_0$ . The  $a$ -value

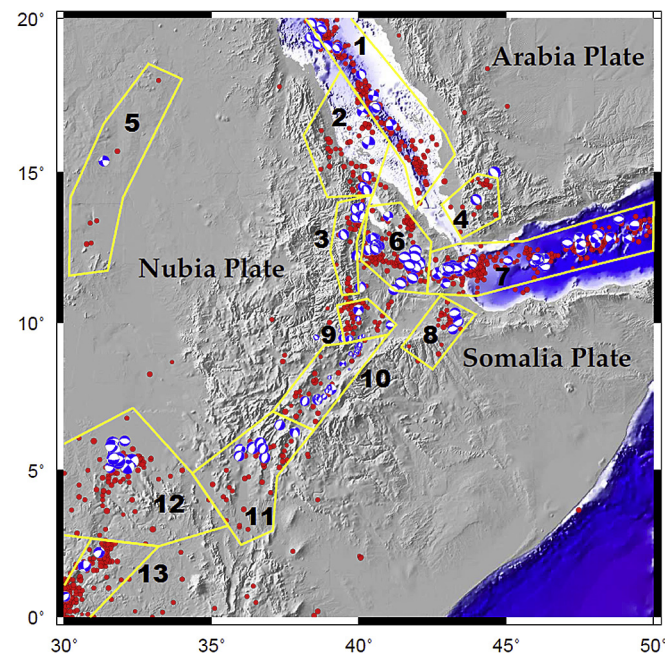


**Fig. 2.** Source zones (yellow polygons) modified from [Hofstetter and Beyth \(2003\)](#) and used in the seismic hazard computations. The blue and white color “beach balls” show fault plane solution plotted on a topographic map and the red dots represent earthquake locations similar to that of [Fig. 1](#).

indicates the overall rate of earthquakes in a region and the  $b$ -value shows the relative ratio of small and large earthquakes (typical  $b$  values are approximately equal to 1) with both values being positive constants. This equation is called the Gutenberg-Richter recurrence law. In our PSHA models we apply a truncated exponential distribution:

$$N(M) = \lambda \frac{e^{-\beta(M-M_0)} - e^{-\beta(M_{max}-M_0)}}{1 - e^{-\beta(M_{max}-M_0)}} \quad M_0 \leq M \leq M_{max} \quad (2)$$

Where  $\beta = b(\ln 10)$ ,  $M_{max}$  is the maximum possible magnitude.  $M_0$  is the minimum or lower bound magnitude and  $\lambda$  is the seismicity rate. This limited magnitude distribution is termed a bounded Gutenberg-Richter recurrence law. [WizmapII](#) software ([Musson, 1998](#)) is used for graphically selecting area polygons for all the 13 zones ([Fig. 2](#), [Table 1](#)) but was also instrumental to estimate the GR parameters  $a$  and  $b$  using the least squares curve fitting technique with at ease guided by the best curve fit and minimum error. However, a single GR recurrence relation curve couldn't be achieved for each of the area sources due to the temporal inhomogeneity of the catalogue which was rather achieved for different time segments. This implies different levels of completeness for the different periods of observation in the catalogue. However, the software prepared by [Kijko and Smit \(2012\)](#) can accommodate temporally inhomogeneous catalogue to produce a pair of  $a$  and  $b$  values for each zone and for the whole time period considered in this study which is handled by a matlab script that generated single  $a$ - and  $b$ -values ([Kijko and Smit, 2012](#)). Using the same matlab script package we also managed to estimate the possible maximum magnitudes for each source zone ([Gibowicz and Kijko, 1994](#); [Kijko and Singh, 2011](#)) and the results are displayed in [Fig. 3](#) and [Table 1](#).

The last model input of interest to consider here is the Ground Motion Prediction Equation (GMPE) also known as attenuation equation or ground-motion model. GMPE is a generic term for an equation providing a statistical estimate of the expected ground motion and its standard deviation due to a given earthquake scenario. The measure of ground-motion provided by a GMPE is typically the 5% damped relative pseudo-spectral acceleration (PSA). The East African rift is one of the places where no strong-motion data have ever been recorded and thus there are no GMPEs estimated or proposed directly based on strong-motion data. Under these circumstances it is a customary practice to assume tectonic analog and extend one of the best known empirical relations as it suits the region of interest ([Douglas et al., 2009](#)). As a result, we adopted [Chiou and Youngs \(2008\)](#) attenuation model in our study which is one of the NGA (Next Generation of Attenuation) equations that have been used for those seismic sources

**Table 1**  
Magnitude-recurrence and maximum magnitudes values for each source zone.

No.	Area Names	$M_0$	$M_{max}$	$b(M_0)$	$\lambda(M_0)$
1	southern Red Sea	4.0	$7.70 \pm 0.20$	$0.79 \pm 0.04$	$3.695 \pm 0.64$
2	eastern Eritrea	4.2	$7.20 \pm 0.18$	$0.78 \pm 0.05$	$1.208 \pm 0.27$
3	western plateau margin	4.0	$5.88 \pm 0.13$	$0.55 \pm 0.04$	$0.540 \pm 0.12$
4	southwestern Yemen	4.1	$6.70 \pm 0.22$	$0.58 \pm 0.05$	$0.885 \pm 0.22$
5	central Sudan	4.5	$5.50 \pm 0.17$	$0.98 \pm 0.24$	$0.181 \pm 0.01$
6	central Afar	4.0	$6.55 \pm 0.16$	$0.69 \pm 0.05$	$1.585 \pm 0.10$
7	Gulf of Aden	4.0	$6.70 \pm 0.12$	$0.69 \pm 0.04$	$5.332 \pm 0.27$
8	Aisha block	4.0	$6.30 \pm 0.15$	$0.62 \pm 0.06$	$0.519 \pm 0.14$
9	Ankober area	4.0	$6.86 \pm 0.17$	$0.93 \pm 0.06$	$1.318 \pm 0.19$
10	Main Ethiopian Rift	4.1	$6.61 \pm 0.15$	$0.60 \pm 0.04$	$0.472 \pm 0.13$
11	southwestern Ethiopia	4.3	$7.20 \pm 0.20$	$0.77 \pm 0.04$	$0.593 \pm 0.12$
12	south Sudan	4.5	$7.70 \pm 9.15$	$0.49 \pm 0.03$	$0.862 \pm 0.11$
13	Albert rift	4.3	$6.50 \pm 0.18$	$0.64 \pm 0.03$	$1.144 \pm 0.18$

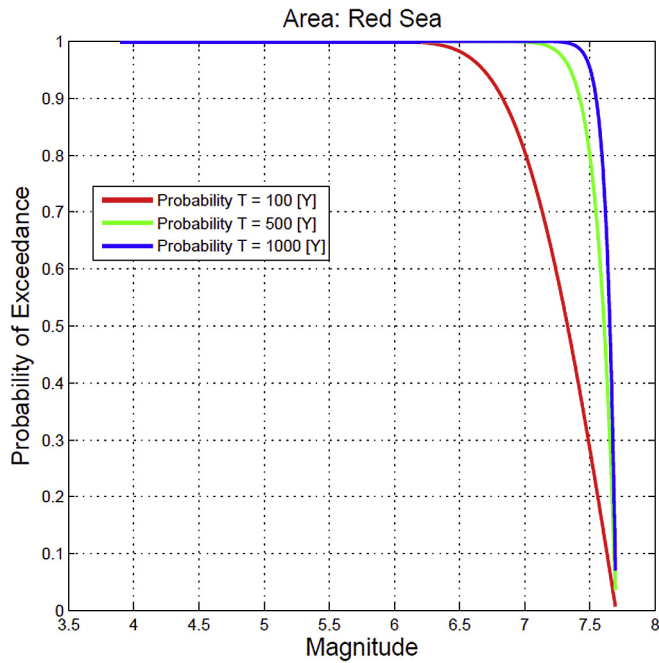


Fig. 3. Probability of Exceedance versus magnitude plot for zone 1 (Red Sea region) as obtained from Kijko and Smit's (2012) Matlab script.

characterized by shallow crustal earthquakes which seems to match the East African rift system pretty well. As most of the earthquake depth is shallow in the East African rift, an average depth of 10 km is used in the hazard calculation of this study. Previous earthquake hazard assessment studies in Ethiopia and neighboring region used similar arguments to adopt attenuation relation from the western United States (Gouin, 1976; Kebede and Van Eck, 1997).

#### 4. Results and discussions

Starting a long time ago, the people in Ethiopia and neighboring region started building villages in and around the active continental rift because of suitability for agriculture like any other part of the East African rift system. Those villages have now developed into modern towns and cities that host multistory buildings with considerable population density. Almost all of the major towns in Ethiopia are located either within the rift floor or near the rift margins where earthquake hazard is relatively high resulting in high earthquake risk in the region. This unintended overlap is noticeable on Fig. 1 which shows the recently compiled distribution of seismicity with major towns and cities that tells a lot even without further analysis of the data. Therefore, the earth science community in the region is expected to provide timely and reliable information for decision makers, planners and engineers on the likelihood and extent of future ground shaking in the area of interest in terms of hazard maps and curves.

This study followed a contemporary PSHA calculation procedure despite the limitation on the availability of suitable data from paleoseismology and historical earthquake catalogue as well as in situ GMPE relations. A new homogenized earthquake catalogue was compiled and updated for the studied region. The catalogue was declustered as required by the Poisson earthquake source model assumption in contrast to previous studies (Gouin, 1976; Kebede and Asfaw, 1996; Kebede and Van Eck, 1997). The Gutenberg-Richter frequency-magnitude relation is applied in each

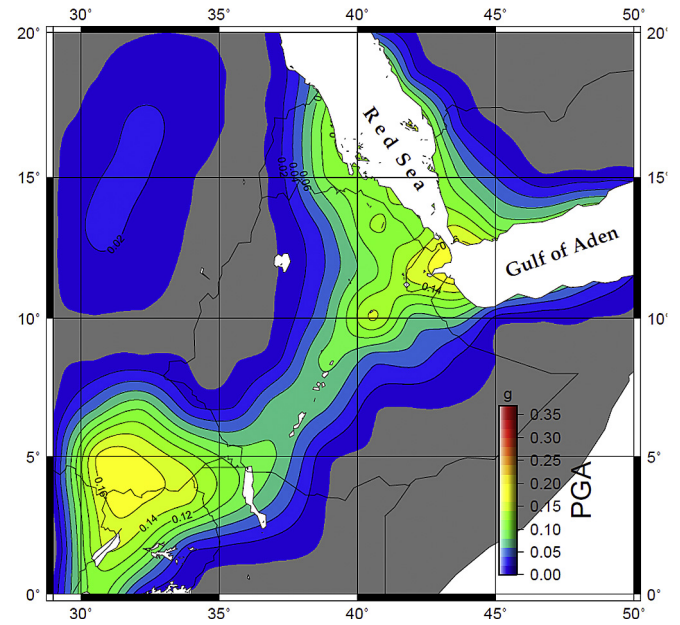


Fig. 4. Horizontal Peak Ground Acceleration seismic hazard map representing rock site condition exceedance rate of 10% within 50 years for Ethiopia and the neighboring region.

of the 13 area sources which were identified from recent seismotectonic understanding of the area (Fig. 2). Though still in the acceptable range of observation that varies from 0.5 to 1.5 (Kebede and Kulhanek, 1994; Wiemer and Benoit, 1996; Ayele and Kulhanek, 1997), b-values summarized in Table 1 are on the lower side which implies the relative occurrence of larger magnitude earthquakes is high. This can also be attributed to under estimation of  $M_0$  due to declustering effect which reduces b-value in hazard calculations as the smaller earthquakes in a cluster are preferentially removed (Gardner and Knopoff, 1974).

The results in this study show horizontal Peak Ground

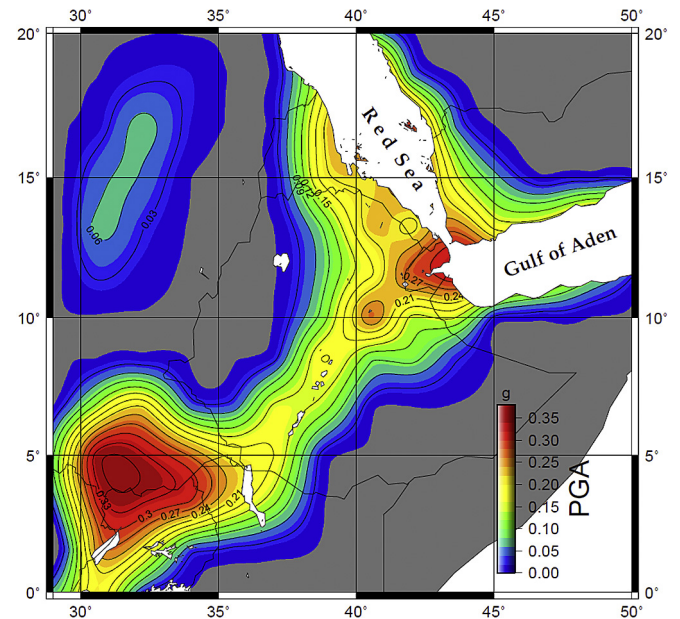
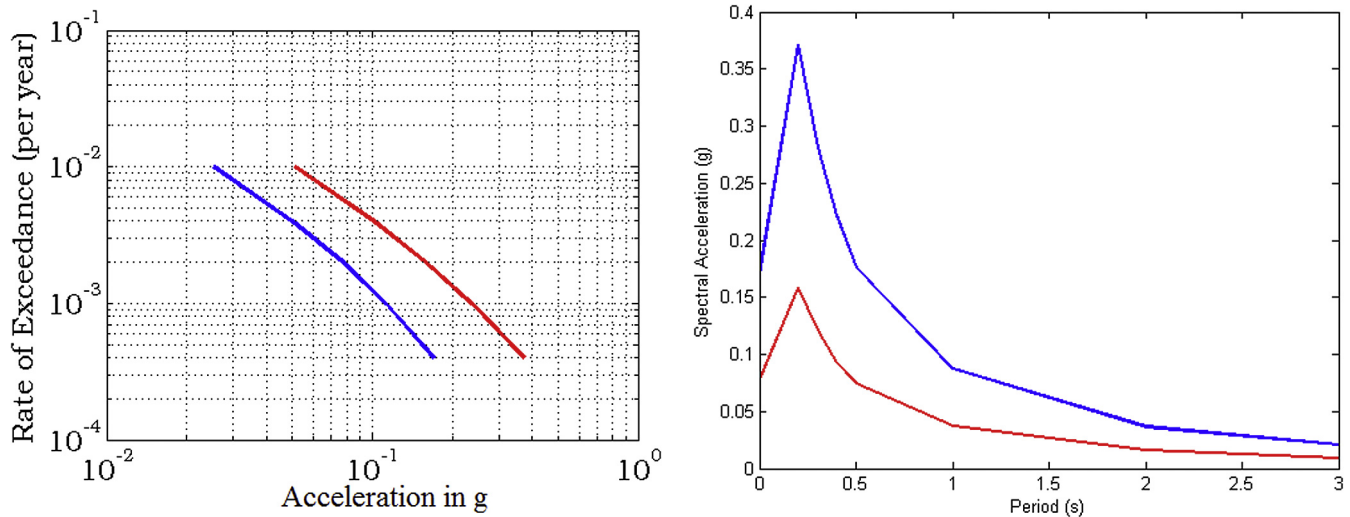


Fig. 5. Horizontal Peak Ground Acceleration seismic hazard map representing rock site condition exceedance rate of 2% within 50 years for Ethiopia and the neighboring region.



**Fig. 6.** Hazard curves for Addis Ababa. (a) PGA rock sites for 475 years (blue) and 2475 years (red) return periods, respectively. (b) Uniform Hazard Spectra (rock sites) 475 and 2475 years return periods, respectively.

Acceleration (PGA) values for 10% and 2% probability of exceedance in 50 years in the spatial window of 0°N to 20°N latitude and 30°E to 50°E longitudes that vary between 0 to 0.18 g and 0–0.35 g (Figs. 4 and 5). The PGA values in this paper are lower than those obtained in previous studies (Gouin, 1976; Kebede and Van Eck, 1997; Midzi et al., 1999) in the region for the length of the return period considered. However, the achieved results are consistent with seismotectonics of the region and obtained by state-of-the-art techniques. The high PGA values observed for the south Sudan seems to be controlled by the May 1990 earthquake sequence while that for Afar region could be influenced by the frequent occurrence of moderate magnitude earthquakes. As developing earthquake hazard model is a process, incorporating more data and refining assumed hazard inputs will improve the map. Hence further investigation is required especially in active fault mapping and characterization from earthquake geology and geodesy. The 10% probability of exceedance in 50 years map (Fig. 4) was recently used for updating the 3rd generation Ethiopian building code (EBCS EN 1998-1:2014). Where seismic design of critical structures including dams is required in the country and the region at large, the more conservative 2% probability of exceedance in 50 years is also included (Fig. 5). Furthermore, studies presented here apply only for hard rock conditions, and hence further investigations that take into account local site conditions and geology are necessary for realistic assessment of the earthquake hazard for an area of interest.

Addis Ababa has posed a concern for earthquake risk as it is one of the fastest growing cities in Africa, located near the active rift margin and being the seat of the African Union and several other international organizations. As a result several tall buildings are emerging in the city. A building is classified as tall if it has a minimum height of 47 m which is roughly about 15 stories (Lew et al., 2008). In today's Addis Ababa, a 15 story building is the average where a special design criterion is required for tall buildings. A provision is made in the criterion for the prevention of collapse of the buildings instead of performance based consideration in time of very rare, large magnitude earthquake. In this case, the conservative 2% probability of exceedance in 50 years may be considered as displayed in Fig. 5 for critical structures. PGA and Spectral Acceleration (SA) hazard curves were generated for Addis Ababa from the current data as displayed in Fig. 6 that will allow the design engineer to have a suit of options to consider. Mammo (2005)

attempted to calculate PGA values for an assumed earthquake of magnitude 6.8 located at 25 km distance from Addis Ababa and obtained 0.294 g, which is too small for the assumed distance and magnitude which might have to do with unrealistic attenuation equation. The hazard curves based on observed data as considered in this study are more reasonable than the assumed calculation in Mammo (2005).

## 5. Conclusions

This paper presents new probabilistic seismic hazard maps produced from a state-of-the-art PSHA study conducted using the classical Cornell McGuire approach for Ethiopia and neighboring region. The PGA values for 10% and 2% probability of exceedance in 50 years in the spatial window of 0°N to 20°N latitude and 30°E to 50°E longitudes vary between 0 and 0.18 g and 0 to 0.35, respectively. The hazard maps were produced for horizontal ground motion at bedrock level. Investigations of the dynamic response of the soil to strong motion will need to be carried out to determine the effects of soil structure on the calculated bedrock ground motion. The evaluation of surface level PSHA is of very high importance in the engineering design which needs more characterization on site conditions at least for economically important cities. As developing earthquake hazard model is a process, incorporating other hazard inputs like active faults, site effects, earthquake geology and other relevant data will improve the map and hence further multidisciplinary investigations (e.g., logic tree considerations) are required.

## Acknowledgements

This work has been carried out at the Institute of Geophysics Space Science and Astronomy of Addis Ababa University, Ethiopia and the International Centre for Theoretical Physics (ICTP), Trieste, Italy under the associate schemes. Mario Ordaz and Roger Musson deserve appreciation, respectively, for making CRISIS2012 and WIZMAP II software freely available for users. I wish to thank Andrzej Kijko for providing matlab scripts for statistical earthquake catalogue analysis. The International Science Program of Uppsala University provided financial assistance. Most of the Figures have been plotted with GMT (Wessel and Smith, 1995).

## Appendix

Potentially destructive earthquakes in the Horn of Africa Region that have been instrumentally recorded with magnitude  $M_w \geq 6.2$ .

No.	Date	Origin Time (GMT)	Latitude	Longitude	Depth (km)	Mag. ( $M_w$ )	Place names
1	1845 02 12		12.25	39.00	10.0	6.5	
2	1854 02 15	03:00	12.80	39.00	10.0	6.3	
3	1903 06 04	14:56	02.00	31.00	10.0	6.4	
4	1906 08 25	11:54	07.62	40.22	10.0	6.6	
5	1906 08 25	13:47	07.41	40.81	10.0	6.8	
6	1912 07 09	08:18	03.33	33.56	10.0	6.8	
7	1913 09 16	11:56	06.00	36.50	10.0	6.2	
8	1915 05 21	04:18	06.00	31.00	10.0	6.6	
9	1915 09 23	08:14	14.48	38.68	10.0	6.8	
10	1919 06 30	07:26	05.58	36.72	10.0	6.5	
11	1928 01 06	19:31	00.34	35.86	15.0	6.8	
12	1928 01 10	02:25	00.38	35.41	15.0	6.2	
13	1937 11 30	12:57	04.93	36.67	10.0	6.8	
14	1938 09 27	02:31	10.45	40.30	15.0	6.3	
15	1950 08 02	13:50	14.52	39.72	15.0	6.2	
16	1955 09 04	22:12	01.80	30.60	10.0	6.3	
17	1960 07 14	18:39	07.00	37.50	10.0	6.3	
18	1961 03 11	08:41	11.65	43.06	10.0	6.2	
19	1961 06 01	23:29	10.46	39.71	12.0	6.5	
20	1961 06 02	04:51	10.16	39.76	10.0	6.2	
21	1961 11 12	02:15	00.60	29.50	10.0	6.3	
22	1967 03 28	02:41	19.90	38.70	12.0	7.2	
23	1977 12 28	02:45	16.54	40.32	13.0	6.6	
24	1982 12 13	09:12	14.64	44.30	12.0	6.2	
25	1987 10 25	16:46	05.35	36.85	15.0	6.2	
26	1989 08 21	01:09	11.78	41.82	13.0	6.4	
27	1990 05 20	02:22	05.14	32.18	15.0	7.2	
28	1990 05 24	19:34	05.36	31.94	10.0	6.4	
29	1990 05 24	20:00	05.30	31.89	16.0	7.0	
31	1990 07 09	15:11	05.36	31.67	13.0	6.2	
32	1992 03 05	08:55	11.47	42.86	07.0	6.2	

## References

- Asfaw, L.M., 1986. Catalogue of Ethiopian earthquakes, earthquake parameters, strain release and seismic risk. May, 1988. In: Woldeyes, G. (Ed.), Proc. SAREC-ESTC Conference on Research Development and Current Research Activities in Ethiopia, pp. 252–279.
- Ayele, A., 1995. Earthquake Catalogue of the Horn of Africa for the Period 1960–1993. Seismology Department, Uppsala University, pp. 1–9. Report 3.
- Ayele, A., Kulhanek, O., 1997. Spatial and temporal variation of seismicity in the horn of Africa from 1960 to 1993. *Geophys. J. Int.* 130, 805–810.
- Ayele, A., Jacques, E., Kassim, M., Kidane, T., Omar, A., Tait, S., Nercessian, A., de Chaballier, J.-B., Kinget, G., 2007. The volcano seismic crisis in Afar, Ethiopia, starting September 2005. *Earth Planet. Sci. Lett.* 255, 187–197.
- Ayele, A., Keir, D., Ebinger, C.J., Wright, T., Stuart, G.W., Buck, R., Jacques, E., Ogubazgh, G., Sholan, J., 2009. The September 2005 mega-dyke emplacement in the Manda-Hararo (Afar) nascent oceanic rift. *Geophys. Res. Lett.* 36, L20306.
- Chiou, B.S.J., Youngs, R.R., 2008. An NGA model for the average horizontal component of peak ground motion and response Spectra. *Earthq. Spectra* 24 (1), 173–215.
- Chu, D., Gordon, R.G., 1999. Evidence for motion between Nubia and Somalia along the southwest indian ridge. *Nature* 398, 64–67.
- Cornell, C.A., 1968. Engineering seismic risk analysis. *Bull. Seismol. Soc. Am.* 58 (1), 583, 1606.
- Cornell, C.A., 1971. Probabilistic analysis of damage to structures under seismic loads. In: Howells, D.A., Haigh, I.P., Taylor, C. (Eds.), *Dynamic Waves in Civil Engineering: Proceedings of a Conference Organized by the Society of Earthquake Civil Engineering Dynamics*. John Wiley, New York, pp. 473–493.
- Das, R., Wason, H.R., Sharma, M.L., 2011. Global regression relations for conversion of surface wave and body wave magnitudes to moment magnitude. *Nat. Hazards* 59, 801–810.
- DesRoches, R., Comerio, M., Eberhard, M., Walter Mooney, W., Rix, G.J., 2011. Overview of the 2010 Haiti earthquake. *Earthq. Spectra* 27 (S1), S1–S21.
- Dick, H.J.B., Lin, J., Schouten, H., 2003. An ultraslow-spreading class of ocean ridge. *Nature* 426, 405–412.
- Douglas, J., Faccioli, E., Cotton, F., Cauzzi, C., 2009. Selection of Ground-motion Prediction Equations for GEM1. GEM Technical Report. GEM Foundation, Pavia, Italy.
- Ebinger, C., Ayele, A., Keir, D., Rowland, J., Yirgu, G., Wright, T., Belachew, M., Hamling, I., 2010. Length and timescales of rift faulting and magma intrusion: the Afar rifting cycle from 2005 to present. *Annu. Rev. Earth Planet. Sci.* 38, 439–466.
- Field, E.H., Jordan, T.H., Cornell, C.A., 2003. OpenSHA: a developing community-modelling environment for seismic hazard analysis. *Seismol. Res. Lett.* 74, 406–419.
- Gardner, J.K., Knopoff, L., 1974. Is the sequence of earthquakes in southern California, with aftershocks removed, poissonian? *Bull. Seismol. Soc. Am.* 64, 1363–1367.
- Garfunkel, Z., Beyth, M., 2006. Constraints on the structural development of Afar imposed by the kinematics of the major surrounding plates. In: Yirgu, G., Ebinger, C.J., Maquire, P.K.H. (Eds.), *The Afar Volcanic Province within the East African Rift System*, vol. 259. *Geol. Soc. Spec. Publ.*, pp. 23–42, 10.1144/GSL.SP.2006.259.01.04.
- Gibowicz, S.J., Kijko, A., 1994. *An Introduction to Mining Seismology*. Academic Press, San Diego.
- Gouin, P., 1976. Seismic zoning in Ethiopia. *Bull. Geophys. Obs. Ethiop.* 17, 1–46.
- Gouin, P., 1979. Earthquake History of Ethiopia and the Horn of Africa. International Development Research Centre (IDRC), Ottawa, Ont., 258 pp.
- Gutenberg, B., Richter, C.F., 1944. Frequency of earthquakes in California. *Bull. Seismol. Soc. Am.* 34, 185–188.
- Hanks, T.C., Kanamori, H., 1979. A moment magnitude scale. *J. Geophys. Res.* 84 (B5), 2348–2350.
- Hofstetter, R., Beyth, M., 2003. The Afar Depression: interpretation of the 1960–2000 earthquakes. *Geophys. J. Int.* 155, 715–732.
- Kanamori, H., 1977. The energy released in great earthquakes. *J. Geophys. Res.* 82, 2981–2987.
- Keir, D., Ayele, A., et al., 2009. Evidence for focused magmatic accretion at segment centers from lateral dyke injections captured beneath the Red Sea rift in Afar. *Geology* 37, 59–62.
- Kebede, F., Asfaw, L., 1996. Seismic hazard assessment for Ethiopia and the neighboring countries. *SINET. Ethiop. J. Sci.* 19 (1), 15–50.
- Kebede, F., Kulhanek, O., 1994. Spatial and temporal variations of b-values along the East African rift system and southern Red Sea. *Phys. Earth Planet. Inter.* 83, 249–264.
- Kebede, F., Van Eck, T., 1997. Probabilistic seismic hazard assessment for the horn of Africa based on seismotectonic regionalization. *Tectonophysics* 270 (3–4), 221–238.
- Kijko, A., Smit, A., 2012. Extension of the Aki-Utsu b-value estimator for incomplete catalogues. *Bull. Seismol. Soc. Am.* 102 (3), 1283–1287.
- Kijko, A., Singh, M., 2011. Statistical tools for maximum possible earthquake magnitude estimation. *Acta Geophys.* 59, 674–700.
- Lew, M., Naeim, F., Hudson, M. B., and Korin, B. O., 2008. Challenges in specifying ground Motions for design of tall buildings in high seismic regions of the United

- States, Proc. of the 14th World Conference on Eq. Eng., 12–17 October 2008, Beijing, China.
- Mammo, T., 2005. Site-specific ground motion simulation and seismic response analysis at the proposed bridge sites within the city of Addis Ababa, Ethiopia. *Eng. Geo* 79 (3–4), 127–150.
- McClusky, S., Ogubazghi, G., Amleson, A., Healeb, B., Vernant, P., Sholan, J., Fisseha, S., Asfaw, L., Bendick, R., Kogan, L., 2009. Kinematics of the southern red sea–afar triple junction and implications for plate dynamics. *Geophys. Res. Lett.* 37 <http://dx.doi.org/10.1029/2009GL041127>.
- McGuire, R.K., 1976. FORTRAN Computer Program for Seismic Risk Analysis. U.S. Geol. Survey Open-File Report No. 76–67.
- McQuarrie, N., Stock, J.M., Verdel, C., Wernicke, B.P., 2003. Cenozoic evolution of Neotethys and implications for the causes of plate motions. *Geophys. Res. Lett.* 30 (20), 2036. <http://dx.doi.org/10.1029/2003GL017992>.
- Midzi, V., Hlatywayo, D.J., Chapola, L.S., Kebede, F., Atakan, K., Lombe, D.K., Turyomurugyendo, G., Tugume, F.A., 1999. Seismic hazard assessment in eastern and southern Africa. *Ann. DI Geofis.* 42 (6), 1067–1083.
- Musson, R.M.W., 1998. *Wizmapll* (British Geological Survey Internal Report).
- Normile, D., 2012. One year after the devastation, Tohoku designs its renewal. *Science* 335, 1164–1166.
- Ordaz, M., Martinelli, F., Aguilar, A., Arboleda, J., Meletti, C., D'Amico, V., CRISIS, 2012. Program for Computing Seismic Hazard. Instituto de Ingeniería, Universidad Nacional Autónoma de México, p. 2012.
- Richter, C.F., 1935. An instrument earthquake magnitude scale. *Bull. Seismol. Soc. Am.* 25, 1–32.
- Scordilis, E.M., 2006. Empirical global relations converting  $M_s$  and  $m_b$  to moment magnitude. *J. Seismol.* 10, 225–236.
- Stein, S., Geller, R.J., Liu, M., 2012. Why earthquake hazard maps often fail and what to do about it. *Tectonophysics* 562–563, 1–25.
- Wessel, P., Smith, W.H.F., 1995. New version of the generic mapping tools released. *EOS. Trans. Am. Geophys. Un.* 76, 329.
- Wiemer, S., Benoit, J., 1996. Mapping the  $b$ -value anomaly at 100 km depth in the Alaska and New Zealand subduction zones. *Geophys. Res. Lett.* 23, 1557–1560.
- Wright, T.C., Ebinger, C., Biggs, J., Ayele, A., Yirgu, G., Keir, D., Stork, A., 2006. Magma-maintained rift segmentation at continental rupture in the 2005 Afar dyking episode. *Nature* 442, 291–294.